Coastal Ocean Simulation of the Gulf of Thailand: A case study of Finite Volume Coastal Ocean Model

S. Tomkratoke and S. Sirisup
Large-Scale Simulation Research Laboratory
National Electronics and Computer Technology Center
112 Thailand Science Park, Klong 1 Klong Luang Pathumthani 12120 Thailand

Abstract*- The Sunda Shelf is settled in Southeast Asia where it forms a large submerged extension of the continental shelf of mainland Asia. The Sunda shelf includes the Greater Sunda Islands of Borneo, Java and Sumatra and the bulk of the shelf forms the shallow seabed of the South China Sea, the coastal areas of Cambodia, Malaysia Peninsula, Singapore, Borneo, and parts of the coast of Indonesia, Thailand, and Vietnam. This shelf is characterized by complex shoreline and seafloor topography which can result in complicated tidal characteristics. In this work, we aim to gain insightful understanding of mechanism of the tidal wave propagation in this region. To achieve this, we perform simulation with high fidelity for the Gulf of Thailand and nearby areas. The high fidelity includes high resolution bathymetry (30 seconds), finer scale capturing and ability to preserve the realistic, complex coastline and islands. To this end, we employ the finite volume method in our simulation for its geometric flexibility, computational efficiency as well as volume and mass conservation assurance. In the current study, we focus mainly on the tidal dynamic processes in the Sunda shelf region, and we numerically scrutinize exact amphidromic systems as well as the corresponding energy flux of the principal tides (M_2, K_1, S_2 and O_1) in the Sunda shelf of the South China Sea. Comparisons to other numerical and experimental observations have been done.

I. INTRODUCTION

The Sunda shelf covers the southwestern part of the South China Sea in Southeast Asia (Fig. 1). In the sense of historic geology, the Sunda shelf was tectonically stable during the Quaternary [1]. The northwest of the Sunda shelf is boarded to the Central Plain of Thailand (Chao Phraya delta) and the southern and western part is surrounded by a hinterland of high elevation (Borneo, Malaysian Peninsula). The narrowest coastal basin of Sunda shelf is located at the upper north of the Thai Gulf while the larger one is located in the western of the shelf. The seafloor topography of this shelf is quite complex with various geomorphology features such as trench, ridges and small islands (Fig. 1). Dynamics of tides in the Sunda shelf, especially the semidiurnal tides, are complex and the tidal currents may be stronger than the current from deep sea. The characteristic of tidal wave in the Sunda shelf such as the Gulf of Thailand has been receiving some great attention in the oceanography researchers. Besides, the complexity of coastline and the seafloor topography of the Sunda shelf can respond to the tidal wave with the unique character. The most important character of tidal wave is the amphidromic system of each tidal constituent. Its existence, locations together with its corresponding rotating direction of amphidromic points of the major tidal constituents can be identified in a given tidal component. A clearer pattern of the tidal wave can be drawn; otherwise, uncertain or incorrectly determined location of amphidromic point can lead to erroneous co-tidal charts.

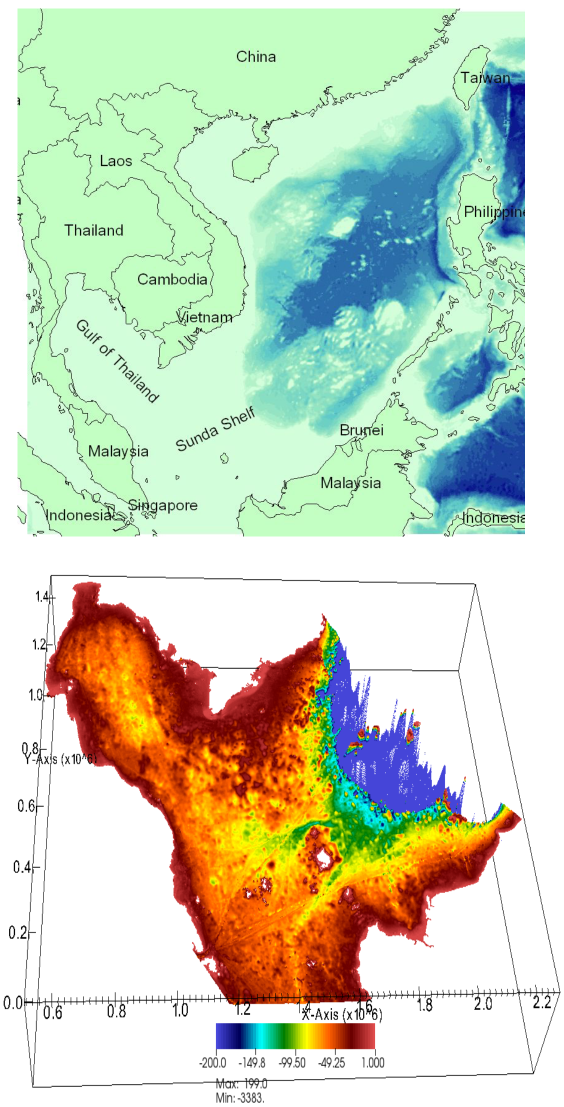

Figure 1. Seafloor topography of the South China Sea (top.) and a 3D plot of the bathymetry of the Sunda shelf (Bottom).

978-1-4244-5222-4/10/$26.00 ©2010 IEEE

For many decades, early investigations of tidal characteristics in the South China Sea have been pursued by numerous oceanographers such as [2], [3], [4] as well as many others. The co-tidal charts for the shelf area drawn by different researchers before the 1980s are actually in great diversity. The discrepancies among the published co-tidal charts have been significantly reduced from 1980s. However, some noticeable differences can still be observed. For example, the recent numerical study by [4] revealed that there is clockwise rotating M_2 amphidromic system with amphidromic point lies in the center of the Gulf of Thailand . They found also that there is one amphidromic system located near the Central Plain of Thailand. The same work also found an S_2 amphidromic system with the amphidromic point lies near the Natuna islands. There are, however, some debates on whether or not there is an S_2 amphidromic system near the Natuna islands. From the recent study through altimetry data in the South China Sea, especially near the aforementioned area. Based on such data, Ref. [5] confirmed that there is no S_2 amphidromic point but rather a nodal line of a standing wave around the Natuna islands instead.

In the present study, apart from confirming the previous statement, we also aim to gain detailed mechanism of tidal wave propagation as well as their amphidromic systems for M_2, S_2, K_1, and O_1 constituents. These constituents are the most important in generating shallow water tides in the shelf areas. In order to obtain the most realistic simulation results with complicated coastlines, islands as well as well represented complex bathymetry; the investigation will be based on simulation using the finite volume method.

II. COMPUTATIONAL DETAILS

The governing equations used in the present study are the boussinesq, hydrostatic approximations of the primitive equations of momentum and (water) momentum conservation which can be written in Cartesian coordinates as below:

$$\frac{\partial u}{\partial t}+u\frac{\partial u}{\partial x}+v\frac{\partial u}{\partial y}-fv=-\frac{1}{\rho_0}\frac{\partial p_a}{\partial x}-g\frac{\partial \eta}{\partial x}+\frac{\partial}{\partial \mathrm{x}}\left(N_h\frac{\partial u}{\partial \mathrm{x}}\right)+\frac{\partial}{\partial \mathrm{y}}\left(N_h\frac{\partial u}{\partial \mathrm{y}}\right)-\frac{\tau_{bx}}{\rho_0(h+\eta)} \quad (1)$$

$$\frac{\partial v}{\partial t}+u\frac{\partial v}{\partial x}+v\frac{\partial v}{\partial y}+fu=-\frac{1}{\rho_0}\frac{\partial p_a}{\partial y}-g\frac{\partial \eta}{\partial y}+\frac{\partial}{\partial \mathrm{x}}\left(N_h\frac{\partial v}{\partial \mathrm{x}}\right)+\frac{\partial}{\partial \mathrm{y}}\left(N_h\frac{\partial v}{\partial \mathrm{y}}\right)-\frac{\tau_{by}}{\rho_0(h+\eta)} \quad (2)$$

$$\frac{\partial \eta}{\partial t}+\frac{\partial (uh)}{\partial x}+\frac{\partial (vh)}{\partial y}+\frac{\partial (u\eta)}{\partial x}+\frac{\partial (v\eta)}{\partial y}=0 \quad (3)$$

where u and v are the dept-averaged currents in the x and y directions. η is the sea surface elevation, h is the undisturbed depth, f is the Coriolis parameter, g is the acceleration due to gravity, p_a is the atmospheric pressure at the sea level, ρ_0 is the water density, N_h is the horizontal eddy viscosity coefficient and τ_{bx}, τ_{by} are the bottom friction stresses in the x and y directions, respectively. We employ the unsteady finite volume coastal ocean model (FVCOM), to simulate the propagation of tidal waves form the four major M_2, K_1, S_2 and O_1 constituents. FVCOM solves the governing equations by using a flux calculation integrated over each model grid control volume with mode-splitting method to external and internal mode time steps to accommodate the faster and slower barotropic and baroclinic responses. More detailed descriptions of FVCOM code can be found in Ref. [6] and [7]. The computational domain and the bathymetry are showed in Fig 2. The domain is set up at the area along latitude 1.35 to 13.53 degree north and longitude 99.27 to 101.86 degree east (141030N to 1496482N and 519691E to 1875413E in UTM datum) covered the Sunda shelf the South China Sea.

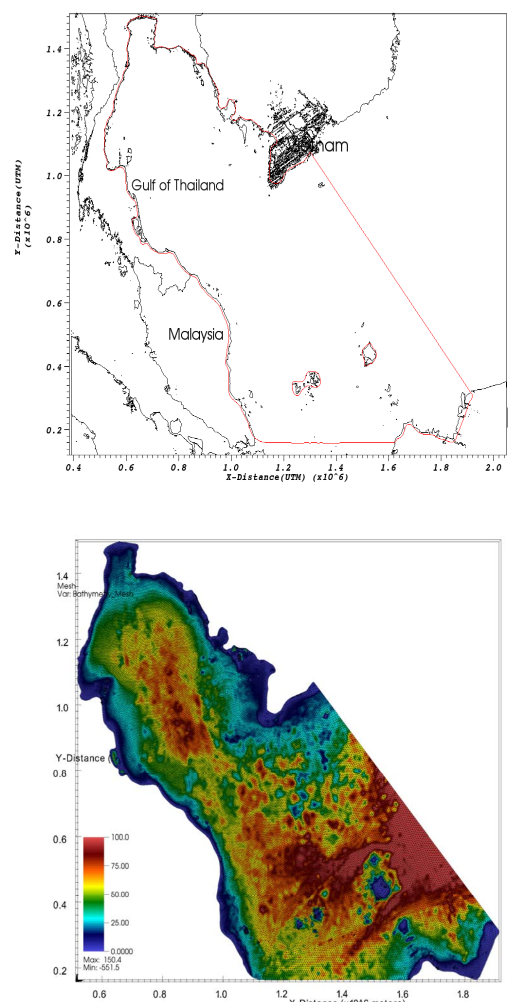

Figure 2. Computational domain (left) and mesh overlaid bathymetry (right).

The domain is decomposed into 70,000 triangular elements; here, the high fidelity bathymetric data with the resolution of 30 seconds from GEBCO [8] is used. The coastlines and the bathymetry near the coast are also enhanced with the electronic nautical charts from the Hydrographic department of the royal Thai navy. The boundary conditions at the open boundaries (the edge of Sunda shelf and Karimata Strait) are prescribed with amplitude and phase information of each constituent derived from OTIS [9]. The resolution dependency will be studied by measuring of the phase and amplitude from the present mesh and those from the refined one. The effect of bottom drag coefficient to the propagation of the tidal wave will be also investigated with value in the range of 0.002 to 0.004.

III. Results and Discussion

A. Tidal stations validation

The results of the simulation from the finite volume coastal model are compared to those observation data obtained from tidal stations around the Gulf of Thailand. The comparison results for the major semi-diurnal tides are given in Table I,II and those for the major diurnal tides are given in Table III, IV. Here, follow Ref [13], we also calculate differences between their amplitudes and phase lags as distances in the complex plane

$$d = \sqrt{(A_{ob}\cos(g_{ob}) - A_{sim}\cos(g_{sim}))^2 + (A_{ob}\sin(g_{ob}) - A_{sim}\sin(g_{sim}))^2} \quad (4)$$

where A_{ob},g_{ob}, A_{sim} and g_{sim} are the observed and simulated amplitudes (cm) and phase lag (degree), respectively.

TABLE I
COMPARISON OF HARMONIC CONSTANT FOR SEMI-DIURNAL TIDE (M_2)

Name	M_2				
(Lat,Long)	A_{ob}	g_{ob}	A_{sim}	g_{sim}	d
Rayong (12º39´,101º16´)	13.7	97.1	13.6	66	7.3
Prasae (12º41´,101º42´)	11.3	74.8	14.5	45.6	7.2
Laemngob (12º10´,102º23´)	10.7	31.7	14.5	37.1	4.0
Langsuan (9º56´,99º9´)	14.2	316.7	9.4	353.0	8.6
Panang (8º21´,100º12´)	17.0	0.7	14.4	287.8	18.7
Sichol (9º00´,99º55´)	15.7	305.2	11.5	269.8	9.1

From Table I-IV, we observe that the amplitudes of the simulation results of all constituents are very close to those of the observation data except for those stations in the south of Thailand in the case of M_2 and K_1. The averaged difference in phase lag of all stations is 34,37,20,22 degrees for M_2, S_2, K_1, O_1, respectively. Overall, we have observed that the simulation results of semi-diurnal tides (averaged d = 9.1 and 4.6 for M_2, S_2) are better that those of diurnal tides (averaged d = 13.9 and 11.1 for K_1, O_1) and the predictions for the northern regions are better than those for the southern regions.

TABLE II
COMPARISON OF HARMONIC CONSTANT FOR SEMI-DIURNAL TIDE (S_2)

Name	S_2				
(Lat,Long)	A_{ob}	g_{ob}	A_{sim}	g_{sim}	d
Rayong (12º39´,101º16´)	6.1	166.0	5.2	130.5	3.5
Prasae (12º41´,101º42´)	5.1	130.9	5.8	111.3	2.0
Laemngob (12º10´,102º23´)	6.4	86.3	5.9	103.6	1.9
Langsuan (9º56´,99º9´)	9.6	27.9	3.6	65	7.1
Panang (8º21´,100º12´)	6.0	76.3	2.0	351.2	7.9
Sichol (9º00´,99º55´)	7.1	16.5	4.5	327.0	5.35

TABLE III
COMPARISON OF HARMONIC CONSTANT FOR DIURNAL TIDE (K_1)

Name	K_1				
(Lat,Long)	A_{ob}	g_{ob}	A_{sim}	g_{sim}	d
Rayong (12º39´,101º16´)	56.7	162.0	58.5	148.4	14.4
Prasae (12º41´,101º42´)	52.9	163.5	55.5	145.4	17.2
Laemngob (12º10´,102º23´)	48.9	156.6	53.7	143.8	12.36
Langsuan (9º56´,99º9´)	47.7	179.5	48.9	163.9	13.21
Panang (8º21´,100º12´)	24.0	223.8	19.6	185.8	14.7
Sichol (9º00´,99º55´)	29.2	189.0	23.7	167.3	11.35

TABLE IV
COMPARISON OF HARMONIC CONSTANT FOR DIURNAL TIDE (O_1)

Name	O_1				
(Lat,Long)	A_{ob}	g_{ob}	A_{sim}	g_{sim}	d
Rayong (12º39´,101º16´)	39.2	103.5	39.1	86.9	11.3
Prasae (12º41´,101º42´)	38.1	103.1	37.4	84.6	12.1
Laemngob (12º10´,102º23´)	36.1	99.0	36.4	83.2	9.97
Langsuan (9º56´,99º9´)	34.7	117.8	34.0	100.7	10.2
Panang (8º21´,100º12´)	19.1	160.1	16.5	116.5	13.4
Sichol (9º00´,99º55´)	22.6	126.4	18.8	101.7	9.6

B. Comparison to prior solutions

The amphidromic systems in the Gulf of Thailand for M_2, S_2, K_1 and O_1 constituents are depicted in Fig. 3 and Fig. 4, respectively. As revealed in Fig. 3 and 4, the pattern of co-tidal lines for both case of semi-diurnal and diurnal tides are in good agreement to the results of [4, 12] with some exceptions for [4]. The amphidromic point for M_2 is found near the central of the Gulf of Thailand and rotating in clockwise direction. We have found that our simulations also produce the nodal band oriented in west-east direction near the upper-north of the Gulf of Thailand meanwhile there is an amphidromic point [4], we will fully describe this behavior in next section. In [4], the amphidromic system for S_2 constituent is rather similar to that of M_2 but the an amphidromic point with counterclockwise rotating fashion shifted Eastward to the Ca Mau Peninsula, however, the tidal regime in the upper-north of the Gulf of Thailand remains the nodal band. Nevertheless, for S_2 amphidromic system, we have rather in our simulations find that, there is the nodal band of S_2 instead of the amphidromic point along the southern part of the Gulf of Thailand. An amphidromic point with rotating clockwise direction is found close to that found in the M_2 amphidromic system. We thus make a comparison to other results to justify this mismatch for the case of S_2. We have found that our result is actually in good agreement to the solution from [9,12] and especially, [5]. The rotating clockwise phase propagation feature of semi-diurnal tide is quite unusual for the Northern Hemisphere. This characteristic will be fully discussed in the next section as well. For the case of diurnal tides, the diurnal tides propagate from the northeast of the South China Sea in to the Gulf of Thailand. The amphidromic systems are found in the middle region of the Gulf but slightly shifted toward the Thailand southern coast and the phase propagation is much closed to [4]. Both systems rotate counterclockwise: this is normal and in good agreement to the Kevin wave theory for the Northern Hemisphere.

C. Tidal dynamics

Here, the mechanism of clockwise phase propagation of semi-diurnal tide and counterclockwise phase propagation of diurnal tide are discussed. For the case of M_2 tide, as we can see in Fig. 3, the clockwise amphidromic system exists close to the tip of Ca Mau Peninsula and far away from the southern coast of Thailand. To explain this mechanism, the effect of sea bed slope, the influence of Coriolis and natural oscillation are to be concerned. The geometry of the Gulf can be characterized by an L shape channel with the longest extension is in the direction to Zhongsha islands and the deepest bottom locate in the middle, see also [4] and analysis by [11]. Supporting by the bottom slope, the incoming M_2 wave acts as an edge wave and propagates along the southern coast to the northern coast. The propagating edge waves are then reflected at the northern and western coast then the tidal wave along the northern coast decreases its amplitude along the eastern coast due to the effects of the node of natural oscillation along the deepest bottom. On the other hand, the amplitude decreasing ratio of the propagating M_2 tidal wave

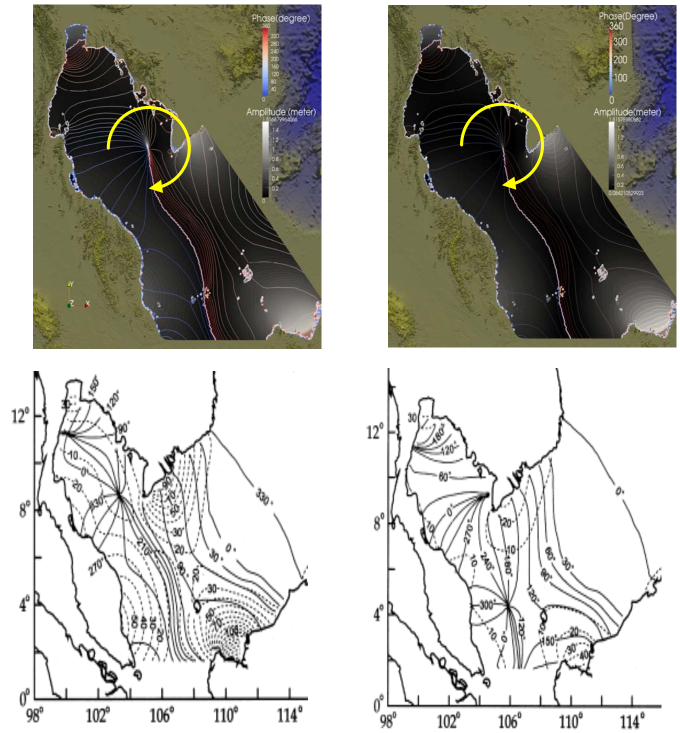

Figure 3. Co-tidal charts for M_2 and S_2 (Left to right).
Top: The present study. Bottom: Work from [4]

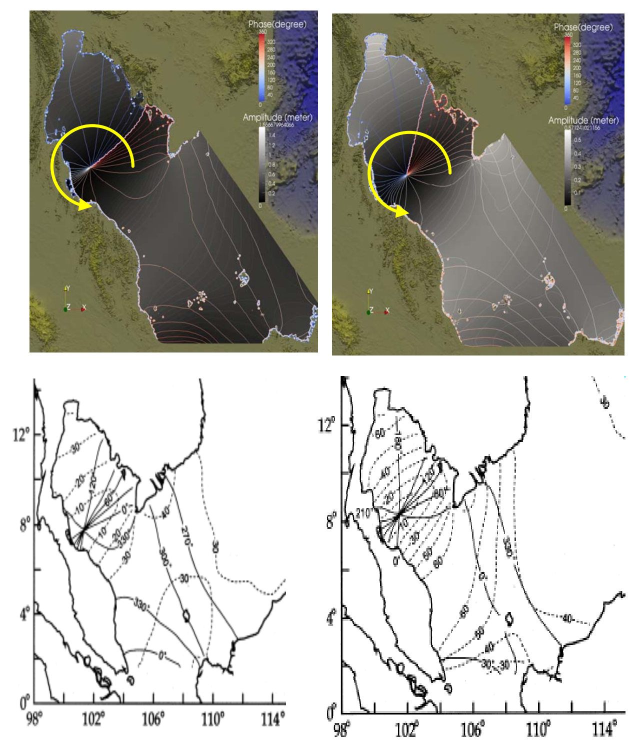

Figure 4. Co-tidal charts for K_1 and O_1 (Left to right).
Top: The present study. Bottom: Work from [4]

along the southern coast is not so large compared to that of the other propagating wave along the northern coast. Therefore, the phase propagation direction of the M_2 amphidromic system is thus clockwise. We also see that there is a large nodal band appears along the deepest bottom slope of the Gulf in the direction to the west tip of Borneo, in this situation, the effects of the interference between the incoming wave from the deep basin and that from the incoming wave from the Karimata Strait is dominated. There is also another nodal band locates near the upper north of the Gulf of Thailand resolved in the current simulation. This nodal band, as oppose to developing into an amphidromic point as found in [4], results from the interference of the northward tidal wave corresponding to the clockwise amphidromic system and the southward reflected wave from the Central plain of Thailand. It is also noted here that the periods of natural oscillations (defined by $T_i=2L_b/i(gH)^{0.5}$, where H is water depth and L_b is width) in south-north and east-west direction in the upper-North Gulf are much smaller than that of the M_2 tide. With this reason, the semi-diurnal tide should not resonate in this region. For the diurnal tides, the phases of K_1 and O_1 tidal wave propagate counterclockwise with effect from the Coriolis force with Kelvin wave's characteristics. This is based on the fact that the periods of the diurnal tides is longer than the period of semi-diurnal tides, therefore the effects of Coriolis force on the K_1 and O_1 tides are much larger than the M_2 and S_2 tides.

D. Tidal energy flux

To gain the understanding of the tidal dynamics of high amplitude tides (M_2 and K_1), the distribution of tidal energy flux in the Sunda shelf is investigated in this section. Following [12], the tidal energy flux can be obtained by the equation below:

$$P = \rho g < U\eta > \quad (4)$$

where ρ is density , U is volume transport vector, which equals the velocity vector multiplied by the water depth, η denotes the sea surface elevation and the operator < > denotes time average. Fig. 5 shows the distribution of the M_2 and K_1 tidal energy flux (in W/m) in the Sunda shelf. As seen in Fig. 5, we have found that the M_2 and K_1 tides do exhibit the different patterns of tidal energy flux distribution which can be summarized as below:

In the case of M_2, the cluster of high energy flux appears near the western coast of Malaysia in Kalimantan Island and near the eastern part of Ca Mao peninsula as well, additionally, we can see also that the energy flux near Sri Chang Island, see Fig 6., in the Gulf of Thailand is amplified. The direction of M_2 tidal energy flux does not conformed to the axis of the (South China Sea) basin but rather deflects toward the main land. This behavior can be explained from the shoaling effect when tidal wave reaches the shallow coast. The dissipation of M_2 energy flux is tightly related to the pattern of amphidromic system which can be expressed as the amplifying and loosing of tidal energy correspond to the nodal and anti-nodal region in Fig 3.

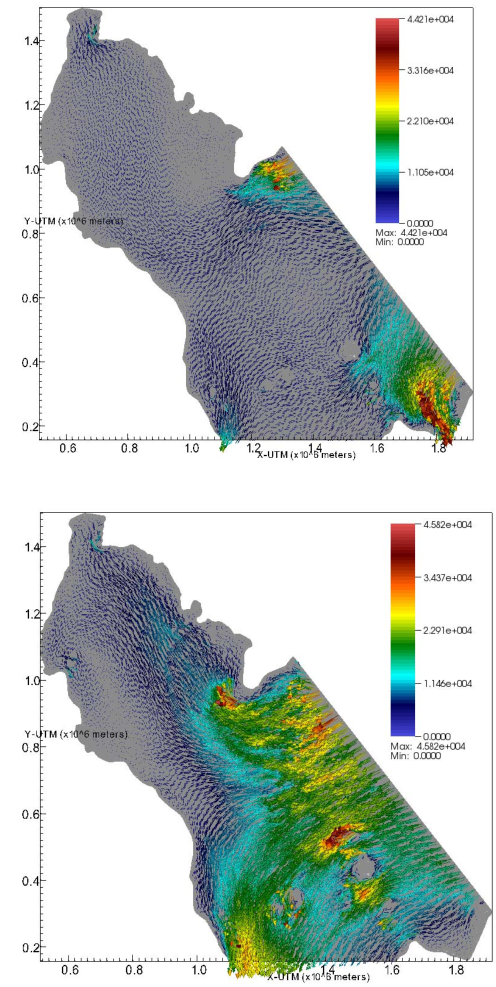

Figure 5. Energy flux for M_2 (top) and K_1 (bottom)

For K_1 tide, the large spreading of high energy flux is found along the Sunda edge and the direction is southwestward conformed to the axis of the basin, see Fig. 4. However, K_1 energy flux continues to dissipate as it enters to shallow continental shelf. Additionally, the regions of highest K_1 energy flux locate near the sea floor trench above Natuna Island and the location beneath the tip of Ca Mao peninsular. From these results, we can conclude that, as K_1 tidal wave enters the Sunda shelf, its energy flux direction is guided mainly by the local seafloor topography and it can be amplified more with sea floor trench where gradients are large.

E. Resolution and bottom friction parameters dependency

In this section, the resolution and bottom friction parameter dependency are discussed. We have found that as the results from the simulation with number of meshes increased from 2 to 5 times as much. The overall profiles (amplitudes and phases variations and profiles of wave propagation) of the amphidromic systems do not show any significant differences. The bottom friction parameter rather plays important role in the change of the magnitude of the amplitudes in the co-tidal charts; however, it does not change any general characteristics of the phases in the co-tidal charts.

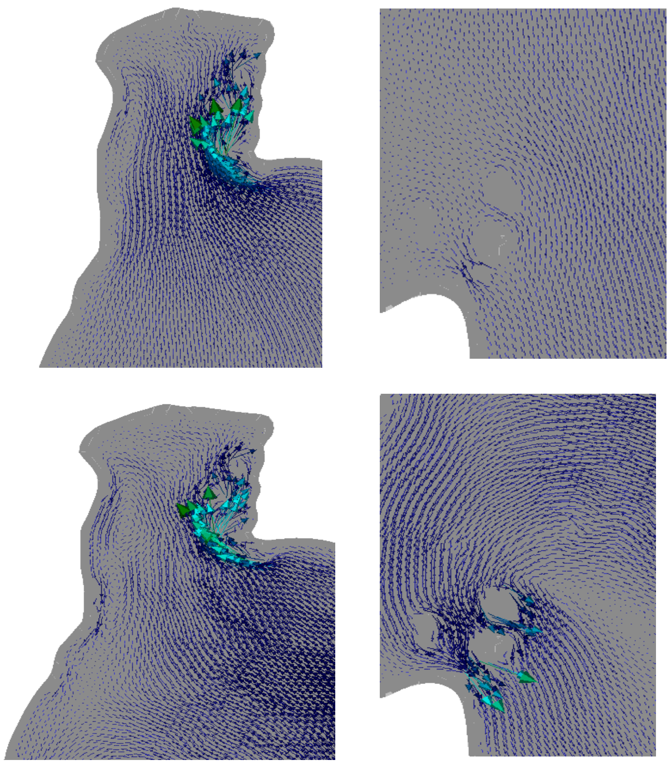

Figure 6. Energy flux for M_2 (top) and K_1 (bottom) focusing on the area of Sri Chang islands (left) and Samui islands (right).

IV. CONCLUSIONS

In this study, the effects of tidal forcing of four major M_2, K_1, S_2 and O_1 constituents in the Gulf of Thailand and nearby areas are investigated. The results of the investigation can be summarized as follows:

1. The effects of the bottom slope, the period of the incoming wave tides and the natural oscillation produce clockwise phase propagation for the M_2 and S_2 tides but produce the counterclockwise amphidromic for K_1 and O_1 tides.
2. The M_2 and S_2 tides produce large nodal bands mainly on the deepest bottom of southern part of the Gulf and the narrow nodal band appear near the upper-North of the Gulf of Thailand.
3. The relation between the tidal flux energy of M_2 and its corresponding amphidromic system is found to be stronger that that of the K_1 tide. However, K_1 energy flux can be greatly amplified by seafloor topography.

ACKNOWLEDGMENT

The authors would like to express their gratitude to the HPC services from the Thai National Grid Center and Large-Scale Simulation Research Laboratory of National Electronics and Computer Technology center for providing computing resources for this project and to the Marine department and the Hydrographic department of the Royal Thai navy for providing us with the data from tidal stations as well as the electronic nautical charts.

REFERENCES

[1] H.D. Tjia, Sea-level changes in the tectonically stable Malay–Thai Peninsula. *Quat. Int*. 31, pp. 95–101, 1996

[2] A.L. Ye, I.S. Robinson, Tidal dynamics in the South China Sea, *Geophysical Journal of the Royal Astronomical Society* , 72, pp. 691-707. 1983.

[3] M. Yu, Preliminary study of tidal characteristics in the South China Sea (in Chinese), *Acta Oceanologica Sinica*, 6, pp. 293-300, 1984.

[4] G.H. Fang, Y.K. Kwok, K.J.Yu *et al.*, Numerical simulation of principal tidal constituents in the South China Sea, Gulf of Tonkin and Gulf of Thailand , *Contin Shelf Res*, 19, pp. 845-869. 1999

[5] M. Qingwen, Q. Yiquan, S. Ping, Z. Haigang, G. Zijun, Is there any amphidromic point of S_2 constituent around the Natuna Islands in the southern South China Sea?, *Chinese Science Bulletin*,51 Supp. II , pp. 26-30, 2006.

[6] C. Chen, H. Liu, R.C. Beardsley,An Unstructured Grid, Finite-Volume, Three-Dimensional, Primitive Equations Ocean Model: Application to Coastal Ocean and Estuaries, *J. Atmos .Ocean. Technol.*, 20 (1), pp. 159-186, 2003 .

[7] Chen C., Huang H., Beardsley R.C., Liu H., Xu Q., Cowles, Technical Report-06-0602, 315 pp., School of marine Science and Technology, University of Massachusetts-Dartmouth, New Bedford, MA.,2006.

[8] IOC, IHO and BODC, 2003, "Centenary Edition of the GEBCO Digital Atlas", published on CD-ROM on behalf of the Intergovernmental Oceanographic Commission and the International Hydrographic Organization as part of the General Bathymetric Chart of the Oceans; British Oceanographic Data Centre, Liverpool.

[9] G.D. Egbert and S. Y. Erofeeva, Efficient Inverse Modeling of Barotropic Ocean Tides, *Journal of Atmospheric and Oceanic Technology*, 19 (2), pp. 183-204, 2002.

[10] C. Garrett, Tides in gulfs. *Deep-Sea Research*, 22, pp. 23–35., 1975.

[11] T. Yanagi and T. Takao, Clockwise Phase Propagation of Semi-Diurnal Tides in the Gulf of Thailand, *Journal of Oceanography*, Vol. 54 (2), pp. 143-150,1997.

[12] T. Zu, J. Gan, S. Y. Erofeeva, Numerical study of the tide and tidal dynamics in the South China Sea, *Deep Sea Research I*, 55, pp. 137-154,2008

[13] M.G.G. Foreman, R.F. Henry, R.A. Walters, V.A. Ballantyne,, A finite element model for tides and resonance along the north coast of British Columbia.*Journal of Geophysical Research* 98, pp. 2509–2531, 1993.